Biophysical Journal, Volume 98

Supporting Material

Autoregulation of ROS via UCP control

William J. Heuett and Vipul Periwal

Supplemental Figure Legends

Figure S1.

Uniporter Ca^{2+}-transport rate, computed as $\tilde{J}_{\rm uni}$ (dashed curves) and $J_{\rm uni}$ (solid curves), for physiological (A) concentrations of intracellular Ca^{2+} ($\Delta\Psi = 120$mV) and (B) $\Delta\Psi$ ($Ca_{\rm i} = 0.2\mu$M).

Figure S2.

Na^+/Ca^{2+}-exchanger rate, computed as $\tilde{J}_{\rm NaCa}$ (dashed curves) and $J_{\rm NaCa}$ (solid curves), for physiological (A) concentrations of mitochondrial Ca^{2+} ($\Delta\Psi = 120$mV) and (B) $\Delta\Psi$ ($Ca_{\rm m} = 0.2\mu$M).

Figure S3.

$NADH_{\rm m}$ production rate from glucose input, computed as $\tilde{J}_{\rm N,Glu}$ with $ATP_{\rm i} = 1.8$mM (dashed curves) and $J_{\rm N,Glu}$ (solid curves), for physiological concentrations of (A) plasma glucose ($Ca_{\rm m} = 0.2\mu$M) and (B) mitochondrial Ca^{2+} ($Glu = 10$mM).

Figure S4.

H_2O production rate from $NADH_{\rm m}$ oxidation, computed as $\tilde{J}_{\rm O,N}$ (dashed curves) and $J_{\rm O,N}$ (solid curves), for physiological (A) concentrations of $NADH_{\rm m}$ ($\Delta\Psi = 120$mV) and (B) $\Delta\Psi$ ($NADH_{\rm m} = 0.75$mM).

Figure S5.

ATP production rate from the F_1F_0-ATP synthase, computed as $\tilde{J}_{\rm F1F0}$ (dashed curves) and $J_{\rm F1F0}$ (solid curves), for physiological (A) ATP/ADP ratios ($\Delta\Psi = 120$mV) and (B) $\Delta\Psi$ ($ATP_{\rm m} = 5$mM).

Figure S6.

ANT exchange rate, computed as $\tilde{J}_{\rm ANT}$ (dashed curves) and $J_{\rm ANT}$ (solid curves), for physiological (A) ATP/ADP ratios ($\Delta\Psi = 120$mV) and (B) $\Delta\Psi$ ($ATP_{\rm m} = 5$mM).

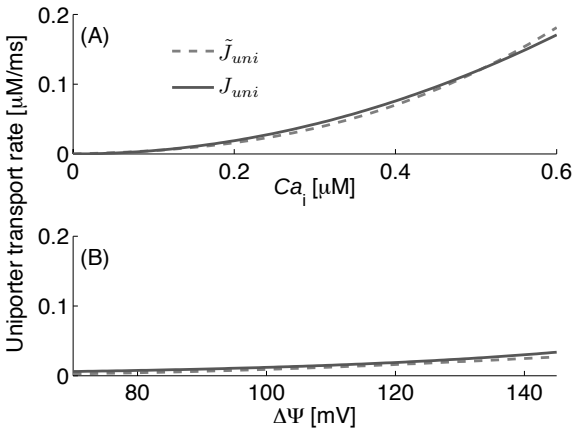
0.2
0.1
0
(A)
$\tilde{J}_{uni}$
J_{uni}
0
0.2
0.4
0.6
Ca_i [μM]
Uniporter transport rate [μM/ms]
0.2
0.1
0
(B)
80
100
120
140
ΔΨ [mV]

Figure S1:

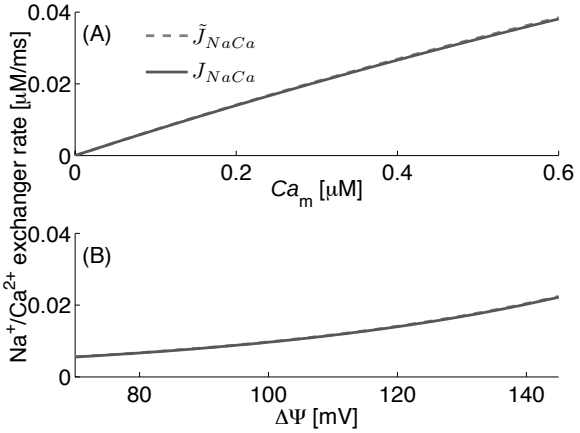
0.04
(A)
$\tilde{J}_{NaCa}$
J_{NaCa}
0.02
0
0
0.2
0.4
0.6
Ca_m [μM]
0.04
(B)
0.02
0
80
100
120
140
ΔΨ [mV]
Na^+/Ca^{2+} exchanger rate [μM/ms]

Figure S2:

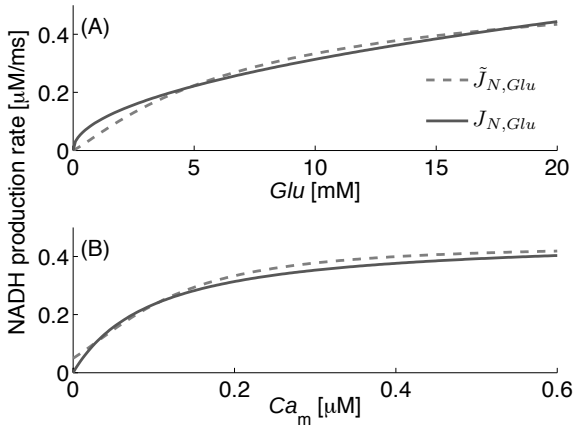
(A)
0.4
0.2
0
0
5
10
15
20
Glu [mM]
$\tilde{J}_{N,Glu}$
$J_{N,Glu}$
NADH production rate [μM/ms]
(B)
0.4
0.2
0
0
0.2
0.4
0.6
Ca_m [μM]

Figure S3:

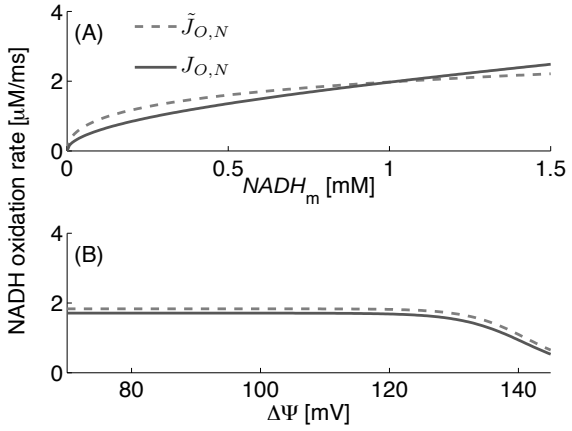
(A)
$\tilde{J}_{O,N}$
$J_{O,N}$
NADH oxidation rate [μM/ms]
4
2
0
0
0.5
1
1.5
$NADH_m$ [mM]
(B)
4
2
0
80
100
120
140
ΔΨ [mV]

Figure S4:

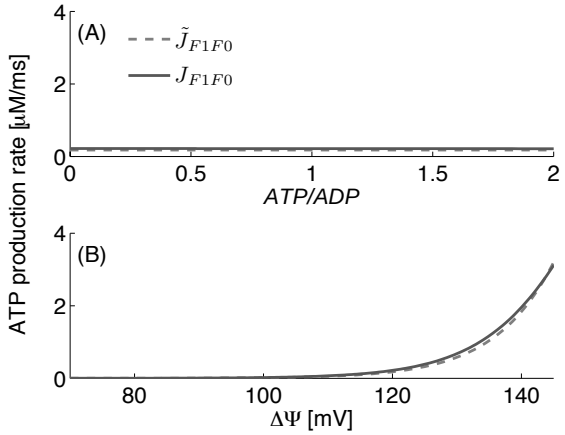
(A)
$\tilde{J}_{F1F0}$
J_{F1F0}
4
2
0
0
0.5
1
1.5
2
ATP/ADP
ATP production rate [μM/ms]
(B)
4
2
0
80
100
120
140
ΔΨ [mV]

Figure S5:

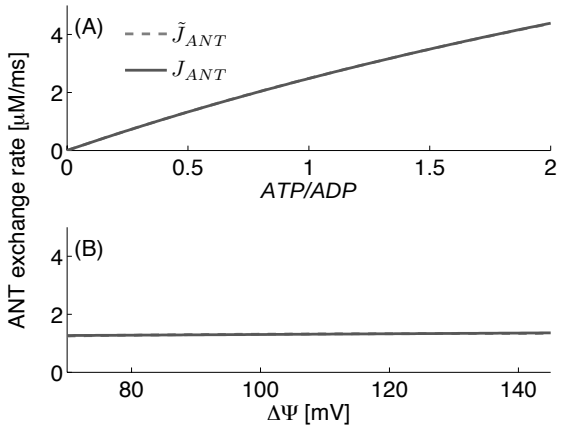
(A)
$\tilde{J}_{ANT}$
J_{ANT}
4
2
0
0
0.5
1
1.5
2
ATP/ADP
(B)
4
2
0
80
100
120
140
ΔΨ [mV]
ANT exchange rate [μM/ms]

Figure S6: